DETAILED TOPOGRAPHIC AND MORPHOMETRIC ANALYSIS OF LYOT'S CENTRAL PEAK GULLIES. S. D. Hart[1], V. C. Gulick[1], S.T. Ishikawa[1], C. J. Barnhart[2] and R. A. Parsons[2], [1]NASA Ames Research Center, M/S 239-20, Moffett Field, CA 94035-1000 (shawn.d.hart@nasa.gov), [2]U.C. Santa Cruz, Earth & Planetary Sciences Department, Earth & Marine Sci., Santa Cruz, CA 95064.

Introduction: Several hypotheses have been proposed to explain the formation of gullies on the surface of Mars. While some have proposed dry mass wasting or exotic fluids [1-3], the detailed landforms found within some Martian gullies appear to require liquid water. Because liquid water is presently unstable on the surface, invoking it as an erosional agent leads to questions about how it arrived at the surface and in what form. Some researchers support shallow or deep water aquifer source regions [4-7], while others propose melting of a shallow ice layer or snowpack deposited during high obliquity periods [8-12]. Gully formation on local topographic highs have been studied previously using MOC images and MOLA profiles to further constrain fluid emplacement mechanisms [13]. In this study, we used HiRISE stereo images and Digital Terrain Maps (DTM) to analyze gully morphology and morphometry on the central peak of Lyot crater. Lyot is a complex crater (~215 km in diameter), located on the edge of the Northern Lowlands just north of the Arabia Terra region (50.4°N, 29.3°E). Our study area consists of three groups of gullies eroded into the central peak's northern, western, and southern slopes.

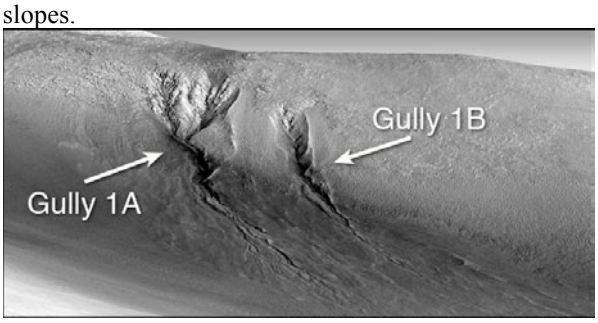

Figure 1. Perspective view of Region 1 gullies 1A and 1B, viewed from the North.

Methods: We used three different methods to measure elevations of gully profiles in HiRISE stereo image pair PSP_008823_2310 and PSP_009245_2310. The first method uses image parallax [14] to obtain relative elevations of features to generate longitudinal profiles of all the major gullies. Spacecraft viewing geometry and the observed parallax between two points in stereo images are used to calculate a change in elevation. First, small objects or features are identified that are common to both images to accurately determine position within the image at the pixel scale with GIS software. Next, the relative shift in position between the pair of points gives a parallax vector, whose orientation is ideally determined by the two camera viewing orientations with its length proportional to the difference in elevation between the objects. In reality, the observed parallax vector orientation deviates slightly from that predicted, allowing us to determine the error in our slope measurement. Typical errors in slope using this method are between 0.5 to 2 degrees over 100 m length scales.

For our second method, we produced a HiRISE DTM using the area-based automatic matching package of the commercial stereo software SOCET SET (® BAE Systems), following the approach developed by Kirk et al. [17]. This DTM was used to make most of the topographic measurements, including longitudinal profiles of all major gullies, volume calculations for gullies 1A, and depth and width measurements to aid discharge calculations. Finally, in our third approach we used MOLA Precision Experiment Data Records (PEDR) data to generate a MOLA DEM within the commercial software Surfer and extracted slope profiles.

Assuming liquid water is responsible for the formation of the gullies, we estimated bank-full fluvial discharges and flow velocities in channels within the two prominent gullies 1A and 1B (Fig. 1). Using the HiRISE stereo image pair and our HiRISE DTM, we measured the widths and depths of the interior sinuous channels in locations where they are well defined. We measured the observed channel geometries, sinuosities, and slopes to estimate discharges using the methods of Kleinhans [15] and Ikeda et al. [16]. A critical assumption in the calculation using Kleinhans' method is that the median grain size cannot currently be resolved at the scale of gully channels from remote sensing. Therefore we used two different median sizes (0.3 mm and 1 cm) that represent likely upper and lower bounds of the grain size. Discharge estimates were calculated for the Region 1 gullies (Fig. 1), the most developed gullies on the central peak.

We also calculated volumes for gullies 1A and 1B, using the HiRISE DTM to create evenly spaced cross-sectional profiles of the gullies. These cross-sectional areas were then calculated using the trapezoidal numerical integration method with a 1m spacing on the x-axis (cross-sectional distance). These areas were then plotted against the distance of the cross-section's location from the top of the gully. Integrating the resulting curve from this method results in a rough approximation of the gully's volume.

Results: Using CTX images of the region, there is evidence of other possible fluvial landforms throughout Lyot crater, including large gullies in the outer western crater wall (~50.7N, 26.5E), smaller gullies located in the southern wall (~48.9N, 28.1E), and possible channel landforms throughout the crater basin that have been previously studied [17].

The gullies are located on poleward and equatorward facing slopes, and trend towards the Northeast in Region 1, towards the East in Region 2, and towards the Southwest in Region 3. The three regions begin at different relative elevations. Region 2 is the lowest, Region 1 has a relative height of ~275 m, and Region 3 is ~340 m above it. None of the gullies appear to originate from a common bedding layer. The alcoves for gullies 1A and 1B have areas of ~616,900 m^2 and ~158,870 m^2 respectively, and have well defined tributary channels eroding into bedrock. Both alcoves are largely free of the loose debris indicative of mass wasting. Areas around these alcoves are covered in polygonal terrain, with polygons ~10m in diameter on average. The interior channels within the gullies both follow sinuous paths and appear to have deeply incised escarpments and point bars present in their meanders. Channel sinuosities are 1.06 for 1A and 1.05 for 1B, while gully wavelengths range from 58-150 m and 66-250 m respectively. The channels on the debris aprons of both gullies display anastamosing patterns, superposition, and gradually transition from negative to positive relief.

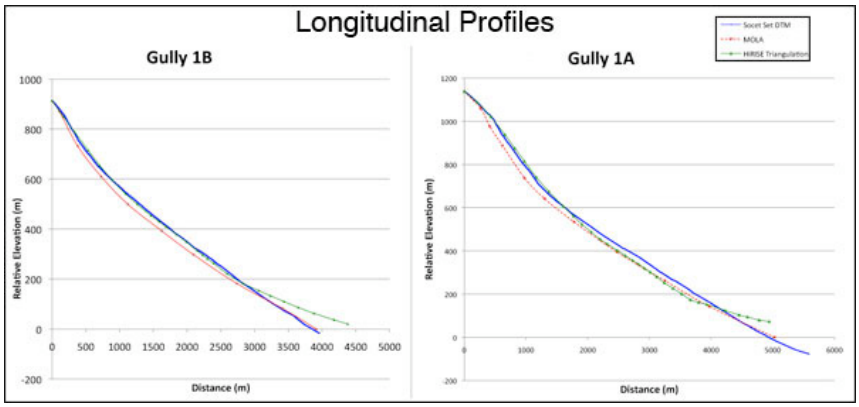

Figure 2. Longitudinal profiles of gullies 1A and 1B, using the three different techniques.

We generated elevation profiles of all six major gullies. Alcove slopes ranged from 16.4° to 29.7°, averaging 22.3° and channel slopes ranged from 11.3° to 20.6°, averaging of 16.1°. The slopes of the debris aprons varied from 8.4° to 16.9°, averaging 11.5°. The MOLA profiles roughly follow the slope and shapes of those done with the HiRISE stereo pair (Fig. 2), giving us confidence in our stereo profiles.

Using Kleinhans method [15], bank-full discharge in gully 1A and 1B ranged from 11.3 to 53.3 m^3/s and from 6.9 m^3/s to 32.1 m^3/s, respectively. Discharge estimates using the Ikeda method [16] ranged from 21.4 m^3/s to 90.9 m^3/s for gully 1A, and from 21.8 to 97.4 m^3/s for gully 1B. The resulting volume calculated for gully 1A is ~12,172,000 m^3, when including the channel and alcove portions.

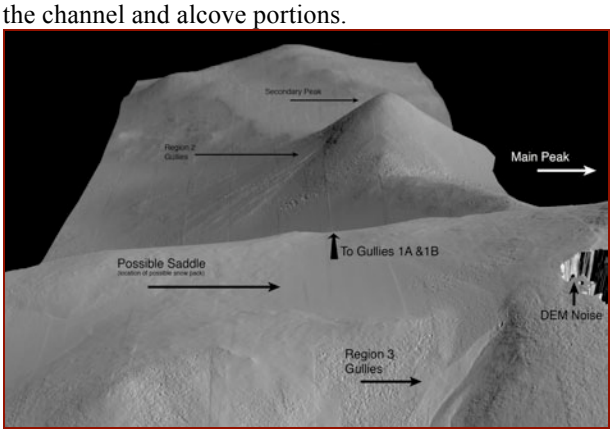

Figure 3. Hill shaded image draped on corresponding DTM of Lyot's central peak, viewed from the south.

Using the HiRISE DTM, it is also possible to study the topography around the gullies. Directly above gullies 1A and 1B is a pole facing topographic saddle (Fig.3). This saddle corresponds to what appears to be a ponding of finer sediment and could represent the location of a past snow pack. Based on our combined morphologic and morphometric studies, we conclude that these gullies are likely formed primarily by fluvial processes. A possible water source may have been from a melting snowpack or ice layer deposited in the uplands above the respective gullies.

References: [1] Musselwhite, D.S. et al. (2001) *Geo.Res.Letters, 28(7),* 1283-85. [2] Treiman, A.H. (2003) *JGR, 108(E4),* 8031. [3] Hugenholtz, C.H. (2008) *Icarus, 197,* 65-72. [4] Malin, M.C. and Edgett, K.S. (2000) *Science, 288*, 2330. [5] Mellon, M.T. and Phillips, R.J. (2001) *JGR, 106(0)*, 1-15. [6] Heldmann, J.L. et al. (2007) *Icarus, 107,* 324-44. [7] Gaidos, E.J. (2001) *Icarus, 153,* 218-23. [8] Costard, F., et al. (2002) *Science, 295*, 110-113. [9] Gilmore, M.S. and Goldenson, N. (2004) *LPSC XXXV,* Abstarct #1884. [10] Hartmann, W.K. et al. (2003) *Icarus, 162,* 259-77. [11] Christensen, P.R. (2003) *Nature, 422,* 45-48. [12] Laskar, J. et al. (2002) *Nature, 419,* 375-77. [13] Dickson, J.L. (2007) *Icarus, 188,* 315-23. [14] Kreslavsky, M.A. (2008) Wrkshp on *Martian Gullies*, *LPI* #8034. [15] Kleinhans, M.G. (2005) *JGR*, *110*, E12003. [16] Ikeda, S., et al. (1981) *J.Fluid Mech., 112*, 363-77. [17] Kirk, R.L. et al. (2008) *JGR* 113, doi: 10.1029/2007JE003000.